Accepted Manuscript
Version of record at: https://doi.org/10.1007/s10444-021-09856-9

A stabilizer-free pressure-robust finite element method for the Stokes equations

Xiu Ye[1], Shangyou Zhang[2]

Shangyou Zhang, szhang@udel.edu
Xiu Ye, xxye@ualr.edu
[1] Department of Mathematics, University of Arkansas at Little Rock, Little Rock, AR 72204, USA
[2] Department of Mathematical Sciences, University of Delaware, Newark, DE 19716, USA

Abstract
In this paper, we introduce a new finite element method for solving the Stokes equa-tions in the primary velocity-pressure formulation using $H(\mathrm{div})$ finite elements to approximate velocity. Like other finite element methods with velocity discretized by $H(\mathrm{div})$ conforming elements, our method has the advantages of an exact divergence-free velocity field and pressure-robustness. However, most of $H(\mathrm{div})$ conforming finite element methods for the Stokes equations require stabilizers to enforce the weak continuity of velocity in tangential direction. Some stabilizers need to tune penalty parameter and some of them do not. Our method is stabilizer free although discontinuous velocity fields are used. Optimal-order error estimates are established for the corresponding numerical approximation in various norms. Extensive numer-ical investigations are conducted to test accuracy and robustness of the method and to confirm the theory. The numerical examples cover low- and high-order approximations up to the degree four, and 2D and 3D cases.

Keywords: Weak gradient, Finite element methods, The Stokes equations, Pressure-robust

Mathematics Subject Classification 2010 Primary · 65N15 · 65N30

Accepted Manuscript
Version of record at: https://doi.org/10.1007/s10444-021-09856-9

1 Introduction

In this paper, we solve the Stokes problem which seeks unknown functions $\mathbf{u}$ and p satisfying

$$-\mu\Delta\mathbf{u} + \nabla p = \mathbf{f} \quad \text{in } \Omega, \tag{1}$$
$$\nabla\cdot\mathbf{u} = 0 \quad \text{in } \Omega, \tag{2}$$
$$\mathbf{u} = 0 \quad \text{on } \partial\Omega, \tag{3}$$

where μ denotes the fluid viscosity and Ω is a polygonal or polyhedral domain in $\mathbb{R}^d$ $(d = 2, 3)$.

The weak form in the primary velocity-pressure formulation for the Stokes problem (1)–(3) seeks $\mathbf{u} \in \boldsymbol{H}_0^1(\Omega)$ and $p \in L_0^2(\Omega)$ satisfying

$$(\mu\nabla\mathbf{u}, \nabla\mathbf{v}) - (\nabla\cdot\mathbf{v}, p) = (\mathbf{f}, \mathbf{v}), \tag{4}$$
$$(\nabla\cdot\mathbf{u}, q) = 0, \tag{5}$$

for all $\mathbf{v} \in \boldsymbol{H}_0^1(\Omega)$ and $q \in L_0^2(\Omega)$.

The Stokes equations have many applications in fluid dynamics and have been studied extensively by researchers. For examples, finite element methods in the primary velocity-pressure formulation have been investigated in [7, 9] for continuous velocity approximations and in [15] for totally discontinuous velocity fields. Between conforming finite element methods and total discontinuous finite element methods, $H(\mathrm{div})$ conforming finite element methods are a good fit for solving the stokes equations with two special features of exact divergence-free velocity field and pressure-robustness, i.e., discrete velocity does not depend on the pressure. Due to these advantages, the $H(\mathrm{div})$ conforming finite element methods have been studied in [6, 18, 19] for the Stokes and the Navier-Stokes equations. Since the $H(\mathrm{div})$ finite element is discontinuous, stabilizers with penalty parameters are required in the formulations in [6, 18, 19]. Other divergence-free and pressure-robust methods are investigated in [8, 11, 13, 16, 23]. More references related to pressure-robustness can be found in [10].

The weak Galerkin (WG) finite element method is an effective and robust numerical technique for the approximate solution of partial differential equations, introduced in [21, 22]. The WG methods use discontinuous piecewise polynomials as approximation on polytopal meshes. The main idea of weak Galerkin finite element methods is the use of weak functions and their corresponding weak derivatives in algorithm design. With the introduction of weak derivative, the WG method has a simple formulation and no need to tune penalty parameters. The Stokes problems and the coupled Stokes-Darcy problems have been studied by the weak Galerkin methods in [4, 5, 12, 20] and by the modified weak Galerkin methods in [14, 17].

In this paper, we develop a new finite element method for solving the Stokes equations in (1)–(3). Like the finite element methods in [6, 19], we use $H(\mathrm{div})$ conforming finite element for the velocity. As a result, this finite element method has exact divergence-free velocity field and is pressure-robust. Unlike the finite element methods in [6, 19], our new finite element method is stabilizer free. Removing stabilizers from the nonconforming finite element methods will simplify formulations and reduce programming complexity. We are able to do so by increasing the degree of polynomials to approximate gradient. The optimal order error estimates are established for the corresponding finite element approximations for velocity and pressure. Our theory and numerical tests demonstrate the pressure-robustness of the method. Extensive numerical examples are tested for the finite elements with different degrees up to P_4 polynomials and for different dimensions, 2D and 3D.

2 Finite element method

We use standard definitions for the Sobolev spaces $H^s(D)$ and their associated inner products $(\cdot,\cdot)_{s,D}$, norms $\|\cdot\|_{s,D}$, and seminorms $|\cdot|_{s,D}$ for $s\ge 0$. When $D=\Omega$, we drop the subscript D in the norm and inner product notation. We also use $L_0^2(\Omega)$ to denote the subspace of $L^2(\Omega)$ consisting of functions with mean value zero.

Let $\mathcal{T}_h$ be a shape regular partition of the domain Ω with mesh size h that consists of triangles/tetrahedrons. Denote by $\mathcal{E}_h$ the set of all flat faces in $\mathcal{T}_h$, and let $\mathcal{E}_h^0=\mathcal{E}_h\backslash\partial\Omega$ be the set of all interior faces.

The space $H(\mathrm{div};\Omega)$ is defined as the set of vector-valued functions on Ω which, together with their divergence, are square integrable; i.e.,

$$H(\mathrm{div};\Omega)=\left\{\mathbf{v}\in[L^2(\Omega)]^d:\ \nabla\cdot\mathbf{v}\in L^2(\Omega)\right\}.$$

For $k\ge 1$ and given $\mathcal{T}_h$, define two finite element spaces for velocity

$$V_h=\left\{\mathbf{v}\in H(\mathrm{div},\Omega):\ \mathbf{v}|_T\in[P_k(T)]^d,\ \forall T\in\mathcal{T}_h,\ \mathbf{v}\cdot\mathbf{n}|_{\partial\Omega}=0\right\}\tag{6}$$

and for pressure

$$W_h=\left\{q\in L_0^2(\Omega):\ q|_T\in P_{k-1}(T)\right\}.\tag{7}$$

Let T_1 and T_2 be two triangles/tetrahedrons in $\mathcal{T}_h$ sharing $e\in\mathcal{E}_h$. For $e\in\mathcal{E}_h$ and $\mathbf{v}\in V_h+\boldsymbol{H}_0^1(\Omega)$, the jump $[\mathbf{v}]$ is defined as

$$[\mathbf{v}]=\mathbf{v}\quad\text{if } e\subset\partial\Omega,\qquad [\mathbf{v}]=\mathbf{v}|_{T_1}-\mathbf{v}|_{T_2}\ \text{ if } e\in\mathcal{E}_h^0.\tag{8}$$

The order of T_1 and T_2 is not essential.

For $e\in\mathcal{E}_h$ and $\mathbf{v}\in V_h+\boldsymbol{H}_0^1(\Omega)$, the average $\{v\}$ is defined as

$$\{\mathbf{v}\}=\mathbf{0}\quad\text{if } e\subset\partial\Omega,\qquad \{\mathbf{v}\}=\frac{1}{2}(\mathbf{v}|_{T_1}+\mathbf{v}|_{T_2})\ \text{ if } e\in\mathcal{E}_h^0.\tag{9}$$

For a function $\mathbf{v}\in V_h+\boldsymbol{H}_0^1(\Omega)$, its weak gradient $\nabla_w\mathbf{v}\in\prod_{T\in\mathcal{T}_h}[P_{k+1}(T)]^{d\times d}$ is defined on each $T\in T_h$ by

$$(\nabla_w\mathbf{v},\ \tau)_T=-(\mathbf{v},\ \nabla\cdot\tau)_T+\langle\{\mathbf{v}\},\ \tau\cdot\mathbf{n}\rangle_{\partial T}\quad\forall\tau\in[P_{k+1}(T)]^{d\times d}.\tag{10}$$

Accepted Manuscript
Version of record at: https://doi.org/10.1007/s10444-021-09856-9

For simplicity, we adopt the following notation,

$$(v, w)_{\mathcal{T}_h} = \sum_{T\in\mathcal{T}_h} (v, w)_T = \sum_{T\in\mathcal{T}_h} \int_T vwd\mathbf{x},$$

$$\langle v, w\rangle_{\partial\mathcal{T}_h} = \sum_{T\in\mathcal{T}_h} \langle v, w\rangle_{\partial T} = \sum_{T\in\mathcal{T}_h} \int_{\partial T} vwds.$$

Then, we have the following simple finite element scheme without stabilizers.

Algorithm 2.1 *A numerical approximation for* (1)–(3) *can be obtained by seeking* $\boldsymbol{u}_h \in V_h$ *and* $p_h \in W_h$ *such that for all* $\boldsymbol{v} \in V_h$ *and* $q \in W_h$,

$$(\mu\nabla_w \boldsymbol{u}_h,\ \nabla_w \boldsymbol{v}) - (\nabla\cdot\boldsymbol{v},\ p_h) = (\boldsymbol{f},\ \boldsymbol{v}), \tag{11}$$

$$(\nabla\cdot\boldsymbol{u}_h,\ q) = 0. \tag{12}$$

Let $\mathbb{Q}_h$ be the element-wise defined L^2 projection onto the space $[P_{k+1}(T)]^{d\times d}$ for $T \in \mathcal{T}_h$.

Lemma 2.1 *Let* $\boldsymbol{\phi} \in \boldsymbol{H}_0^1(\Omega)$, *then on* $T \in \mathcal{T}_h$

$$\nabla_w\boldsymbol{\phi} = \mathbb{Q}_h\nabla\boldsymbol{\phi}. \tag{13}$$

Proof Using (10) and integration by parts, we have that for any $\tau \in [P_{k+1}(T)]^{d\times d}$

$$\begin{aligned}(\nabla_w\boldsymbol{\phi}, \tau)_T &= -(\boldsymbol{\phi}, \nabla\cdot\tau)_T + \langle\{\boldsymbol{\phi}\}, \tau\cdot\mathbf{n}\rangle_{\partial T}\\ &= -(\boldsymbol{\phi}, \nabla\cdot\tau)_T + \langle\boldsymbol{\phi}, \tau\cdot\mathbf{n}\rangle_{\partial T}\\ &= (\nabla\boldsymbol{\phi}, \tau)_T = (\mathbb{Q}_h\nabla\boldsymbol{\phi}, \tau)_T,\end{aligned}$$

which implies the desired identity (13). □

For any function $\varphi \in H^1(T)$, the following trace inequality holds true (see [2, 22] for details):

$$\|\varphi\|_e^2 \leq C\left(h_T^{-1}\|\varphi\|_T^2 + h_T\|\nabla\varphi\|_T^2\right). \tag{14}$$

3 Well posedness

We assume $\mu = 1$ for simplicity. We start this section by introducing two semi-norms $|||\mathbf{v}|||$ and $\|\mathbf{v}\|_{1,h}$ for any $\mathbf{v} \in V_h \cup \boldsymbol{H}_0^1(\Omega)$ as follows:

$$|||\mathbf{v}|||^2 = \sum_{T\in\mathcal{T}_h} (\nabla_w\mathbf{v}, \nabla_w\mathbf{v})_T, \tag{15}$$

$$\|\mathbf{v}\|_{1,h}^2 = \sum_{T\in\mathcal{T}_h} \|\nabla\mathbf{v}\|_T^2 + \sum_{e\in\mathcal{E}_h} h_e^{-1}\|[\mathbf{v}]\|_e^2. \tag{16}$$

It is easy to see that $\|\mathbf{v}\|_{1,h}$ defines a norm in V_h. The following norm equivalence has been proved in [1],

$$C_1\|\mathbf{v}\|_{1,h} \leq |||\mathbf{v}||| \leq C_2\|\mathbf{v}\|_{1,h} \quad \forall \mathbf{v} \in V_h. \tag{17}$$

Define an interpolator Π_h for $\tau \in [H^1(\Omega)]^d$ (see [3]) such that $\Pi_h\tau \in V_h$ and on each $T \in \mathcal{T}_h$

$$(\nabla\cdot\tau,\ v)_T = (\nabla\cdot\Pi_h\tau,\ v)_T \quad \forall v \in P_{k-1}(T). \tag{18}$$

The interpolator Π_h has the following interpolation property for $\tau \in [H^{k+1}(\Omega)]^d$,

$$\sum_{T\in\mathcal{T}_h}\|\tau-\Pi_h\tau\|_T^2 + \sum_{T\in\mathcal{T}_h} h_T^2\|\nabla(\tau-\Pi_h\tau)\|_T^2 \leq Ch^{2(k+1)}\|\tau\|_{k+1}^2. \tag{19}$$

The inf-sup condition for the finite element formulation (11)-(12) will be derived in the following lemma.

Lemma 3.1 *There exists a positive constant β independent of h such that for all $\rho \in W_h$,*

$$\sup_{\boldsymbol{v}\in V_h}\frac{(\nabla\cdot\boldsymbol{v},\rho)}{|||\boldsymbol{v}|||} \geq \beta\|\rho\|. \tag{20}$$

Proof For any given $\rho \in W_h \subset L_0^2(\Omega)$, it is known [9] that there exists a function $\tilde{\mathbf{v}} \in \boldsymbol{H}_0^1(\Omega)$ such that

$$\frac{(\nabla\cdot\tilde{\mathbf{v}},\rho)}{\|\tilde{\mathbf{v}}\|_1} \geq C\|\rho\|, \tag{21}$$

where $C > 0$ is a constant independent of h. By setting $\mathbf{v} = \Pi_h\tilde{\mathbf{v}} \in V_h$, we prove next that the following holds true

$$|||\mathbf{v}||| \leq C\|\tilde{\mathbf{v}}\|_1. \tag{22}$$

It follows from (17), (14) and $\tilde{\mathbf{v}} \in \boldsymbol{H}_0^1(\Omega)$,

$$\begin{aligned}
|||\mathbf{v}|||^2 &\leq C\|\mathbf{v}\|_{1,h}^2 = C\left(\sum_{T\in\mathcal{T}_h}\|\nabla\mathbf{v}\|_T^2 + \sum_{e\in\mathcal{E}_h^0} h_e^{-1}\|[\mathbf{v}]\|_e^2\right)\\
&\leq C\sum_{T\in\mathcal{T}_h}\|\nabla\Pi_h\tilde{\mathbf{v}}\|_T^2 + \sum_{e\in\mathcal{E}_h^0} h_e^{-1}\|[\Pi_h\tilde{\mathbf{v}}-\tilde{\mathbf{v}}]\|_e^2\\
&\leq C\|\tilde{\mathbf{v}}\|_1^2,
\end{aligned}$$

which implies the inequality (22). It follows from (18) that

$$(\nabla\cdot\mathbf{v},\ \rho) = (\nabla\cdot\Pi_h\tilde{\mathbf{v}},\ \rho) = (\nabla\cdot\tilde{\mathbf{v}},\ \rho).$$

Using the above equation, (21) and (22), we have

$$\frac{|(\nabla\cdot\mathbf{v},\rho)|}{|||\mathbf{v}|||} \geq \frac{|(\nabla\cdot\tilde{\mathbf{v}},\rho)|}{C\|\tilde{\mathbf{v}}\|_1} \geq \beta\|\rho\|,$$

for a positive constant β. This completes the proof of the lemma. □

Lemma 3.2 *The weak Galerkin method (11)-(12) has a unique solution.*

Proof It suffices to show that zero is the only solution of (11)-(12) if $\mathbf{f} = \mathbf{0}$. To this end, let $\mathbf{f} = \mathbf{0}$ and take $\mathbf{v} = \mathbf{u}_h$ in (11) and $q = p_h$ in (12). By adding the two resulting equations, we obtain

$$(\nabla_w \mathbf{u}_h,\ \nabla_w \mathbf{u}_h) = 0,$$

which implies that $\nabla_w \mathbf{u}_h = 0$ on each element T. By (17), we have $\|\mathbf{u}_h\|_{1,h} = 0$ which implies that $\mathbf{u}_h = 0$.

Since $\mathbf{u}_h = \mathbf{0}$ and $\mathbf{f} = \mathbf{0}$, the equation (11) becomes $(\nabla\cdot\mathbf{v},\ p_h) = 0$ for any $\mathbf{v} \in V_h$. Then the inf-sup condition (20) implies $p_h = 0$. We have proved the lemma. □

4 Error equations

In this section, we will derive the equations that the errors satisfy. First, we define an element-wise L^2 projection Q_h onto the local space $P_{k-1}(T)$ for $T \in \mathcal{T}_h$. Let $\mathbf{e}_h = \Pi_h \mathbf{u} - \mathbf{u}_h$, $\boldsymbol{\epsilon}_h = \mathbf{u} - \mathbf{u}_h$ and $\varepsilon_h = Q_h p - p_h$.

Lemma 4.1 *Let $\boldsymbol{u} \in [H^2(\Omega)]^d$ and $p \in H^1(\Omega)$. For any $\boldsymbol{v} \in V_h$ and $q \in W_h$, the following error equations hold true,*

$$(\nabla_w \boldsymbol{e}_h,\ \nabla_w \boldsymbol{v}) - (\varepsilon_h,\ \nabla\cdot\boldsymbol{v}) = \ell_1(\boldsymbol{u},\boldsymbol{v}) - \ell_2(\boldsymbol{u},\boldsymbol{v}), \tag{23}$$

$$(\nabla\cdot\boldsymbol{e}_h,\ q) = 0, \tag{24}$$

where

$$\ell_1(\boldsymbol{u},\ \boldsymbol{v}) = \langle \boldsymbol{v} - \{\boldsymbol{v}\},\ \nabla\boldsymbol{u}\cdot\boldsymbol{n} - \mathbb{Q}_h(\nabla\boldsymbol{u})\cdot\boldsymbol{n}\rangle_{\partial\mathcal{T}_h}, \tag{25}$$

$$\ell_2(\boldsymbol{u},\boldsymbol{v}) = (\nabla_w(\boldsymbol{u} - \Pi_h\boldsymbol{u}),\ \nabla_w\boldsymbol{v}). \tag{26}$$

Proof First, we test (1) by $\mathbf{v} \in V_h$ to obtain

$$-(\Delta\mathbf{u},\ \mathbf{v}) + (\nabla p,\ \mathbf{v}) = (\mathbf{f},\ \mathbf{v}). \tag{27}$$

Integration by parts gives

$$-(\Delta\mathbf{u},\ \mathbf{v}) = (\nabla\mathbf{u}, \nabla\mathbf{v})_{\mathcal{T}_h} - \langle\nabla\mathbf{u}\cdot\mathbf{n}, \mathbf{v} - \{\mathbf{v}\}\rangle_{\partial\mathcal{T}_h}, \tag{28}$$

where we use the fact $\langle\nabla\mathbf{u}\cdot\mathbf{n}, \{\mathbf{v}\}\rangle_{\partial T_h} = 0$. It follows from integration by parts, (10) and (13),

$$\begin{aligned}
(\nabla\mathbf{u}, \nabla\mathbf{v})_{\mathcal{T}_h} &= (\mathbb{Q}_h\nabla\mathbf{u}, \nabla\mathbf{v})_{\mathcal{T}_h} \\
&= -(\mathbf{v}, \nabla\cdot(\mathbb{Q}_h\nabla\mathbf{u}))_{\mathcal{T}_h} + \langle\mathbf{v}, \mathbb{Q}_h\nabla\mathbf{u}\cdot\mathbf{n}\rangle_{\partial\mathcal{T}_h} \\
&= (\mathbb{Q}_h\nabla\mathbf{u}, \nabla_w\mathbf{v})_{\mathcal{T}_h} + \langle\mathbf{v} - \{\mathbf{v}\}, \mathbb{Q}_h\nabla\mathbf{u}\cdot\mathbf{n}\rangle_{\partial\mathcal{T}_h} \\
&= (\nabla_w\mathbf{u}, \nabla_w\mathbf{v}) + \langle\mathbf{v} - \{\mathbf{v}\}, \mathbb{Q}_h\nabla\mathbf{u}\cdot\mathbf{n}\rangle_{\partial\mathcal{T}_h}.
\end{aligned} \tag{29}$$

Combining (28) and (29) gives

$$-(\Delta\mathbf{u},\ \mathbf{v}) = (\nabla_w\mathbf{u}, \nabla_w\mathbf{v}) - \ell_1(\mathbf{u}, \mathbf{v}). \tag{30}$$

Accepted Manuscript
Version of record at: https://doi.org/10.1007/s10444-021-09856-9

Using integration by parts and $\mathbf{v} \in V_h$, we have

$$(\nabla p,\ \mathbf{v}) = -(p, \nabla\cdot\mathbf{v})_{\mathcal{T}_h} + \langle p, \mathbf{v}\cdot\mathbf{n}\rangle_{\partial\mathcal{T}_h} = -(p, \nabla\cdot\mathbf{v})_{\mathcal{T}_h} = -(Q_h p, \nabla\cdot\mathbf{v})_{\mathcal{T}_h}. \quad (31)$$

Substituting (30) and (31) into (27) gives

$$(\nabla_w \mathbf{u}, \nabla_w \mathbf{v}) - (Q_h p, \nabla\cdot\mathbf{v})_{\mathcal{T}_h} = (\mathbf{f}, \mathbf{v}) + \ell_1(\mathbf{u}, \mathbf{v}). \quad (32)$$

The difference of (32) and (11) implies

$$(\nabla_w \boldsymbol{\epsilon}_h, \nabla_w \mathbf{v}) - (\varepsilon_h, \nabla\cdot\mathbf{v})_{\mathcal{T}_h} = \ell_1(\mathbf{u}, \mathbf{v}) \quad \forall \mathbf{v} \in V_h. \quad (33)$$

Adding and subtracting $(\nabla_w \Pi_h \mathbf{u}, \nabla_w \mathbf{v})$ in (33), we have

$$(\nabla_w \mathbf{e}_h, \nabla_w \mathbf{v}) - (\varepsilon_h, \nabla\cdot\mathbf{v})_{\mathcal{T}_h} = \ell_1(\mathbf{u}, \mathbf{v}) - \ell_2(\mathbf{u}, \mathbf{v}), \quad (34)$$

which implies (23).

Testing equation (2) by $q \in W_h$ and using (18) give

$$(\nabla\cdot\mathbf{u},\ q) = (\nabla\cdot\Pi_h \mathbf{u},\ q)_{\mathcal{T}_h} = 0. \quad (35)$$

The difference of (35) and (12) implies (24). We have proved the lemma. □

5 Error estimates in energy norm

In this section, we shall establish optimal order error estimates for the velocity approximation $\mathbf{u}_h$ in $|||\cdot|||$ norm and for the pressure approximation p_h in the standard L^2 norm.

It is easy to see that the following equations hold true for $\{\mathbf{v}\}$ defined in (9),

$$\|\mathbf{v} - \{\mathbf{v}\}\|_e = \|[\mathbf{v}]\|_e \quad \text{if } e \subset \partial\Omega, \qquad \|\mathbf{v} - \{\mathbf{v}\}\|_e = \frac{1}{2}\|[\mathbf{v}]\|_e \ \text{ if } e \in \mathcal{E}_h^0. \quad (36)$$

Lemma 5.1 *Let $\boldsymbol{w} \in \boldsymbol{H}^{k+1}(\Omega)$ and $\rho \in H^k(\Omega)$ and $\boldsymbol{v} \in V_h$. Assume that the finite element partition $\mathcal{T}_h$ is shape regular. Then, the following estimates hold true*

$$|\ell_1(\boldsymbol{w},\ \boldsymbol{v})| \le Ch^k |\boldsymbol{w}|_{k+1} |||\boldsymbol{v}|||, \quad (37)$$
$$|\ell_2(\boldsymbol{w},\ \boldsymbol{v})| \le Ch^k |\boldsymbol{w}|_{k+1} |||\boldsymbol{v}|||. \quad (38)$$

Proof Using the Cauchy-Schwarz inequality, the trace inequality (14), (36), and (17), we have

$$\begin{aligned}
|\ell_1(\mathbf{w},\ \mathbf{v})| &= \Big|\sum_{T\in\mathcal{T}_h} \langle \mathbf{v} - \{\mathbf{v}\},\ \nabla\mathbf{w}\cdot\mathbf{n} - \mathbb{Q}_h(\nabla\mathbf{w})\cdot\mathbf{n}\rangle_{\partial T}\Big| \\
&\le C \sum_{T\in\mathcal{T}_h} \|\nabla\mathbf{w} - \mathbb{Q}_h\nabla\mathbf{w}\|_{\partial T} \|\mathbf{v} - \{\mathbf{v}\}\|_{\partial T} \\
&\le C \left(\sum_{T\in\mathcal{T}_h} h_T \|(\nabla\mathbf{w} - \mathbb{Q}_h\nabla\mathbf{w})\|_{\partial T}^2\right)^{\frac{1}{2}} \left(\sum_{e\in\mathcal{E}_h} h_e^{-1} \|[\mathbf{v}]\|_e^2\right)^{\frac{1}{2}} \\
&\le Ch^k |\mathbf{w}|_{k+1} |||\mathbf{v}|||.
\end{aligned}$$

Accepted Manuscript
Version of record at: https://doi.org/10.1007/s10444-021-09856-9

Next we estimate $|\ell_2(\mathbf{w},\mathbf{v})| = |(\nabla_w(\mathbf{w}-\Pi_h\mathbf{w}),\nabla_w\mathbf{v})|$. It follows from (10), integration by parts, (14) and (36) that for any $\mathbf{q}\in[P_{k+1}(T)]^{d\times d}$,

$$
\begin{aligned}
&|(\nabla_w(\mathbf{w}-\Pi_h\mathbf{w}),\mathbf{q})_T|\\
&=|-(\mathbf{w}-\Pi_h\mathbf{w},\nabla\cdot\mathbf{q})_T+\langle\mathbf{w}-\{\Pi_h\mathbf{w}\},\mathbf{q}\cdot\mathbf{n}\rangle_{\partial T}|\\
&=|(\nabla(\mathbf{w}-\Pi_h\mathbf{w}),\mathbf{q})_T+\langle\Pi_h\mathbf{w}-\{\Pi_h\mathbf{w}\},\mathbf{q}\cdot\mathbf{n}\rangle_{\partial T}|\\
&\le\|\nabla(\mathbf{w}-\Pi_h\mathbf{w})\|_T\|\mathbf{q}\|_T+Ch^{-1/2}\|[\Pi_h\mathbf{w}]\|_{\partial T}\|\mathbf{q}\|_T\\
&=\|\nabla(\mathbf{w}-\Pi_h\mathbf{w})\|_T\|\mathbf{q}\|_T+Ch^{-1/2}\|[\mathbf{w}-\Pi_h\mathbf{w}]\|_{\partial T}\|\mathbf{q}\|_T\\
&\le Ch^k|\mathbf{w}|_{k+1,T}\|\mathbf{q}\|_T.
\end{aligned}
\tag{39}
$$

Letting $\mathbf{q}=\nabla_w\mathbf{v}$ in the above equation and taking summation over T, we have

$$|\ell_2(\mathbf{w},\ \mathbf{v})|\le Ch^k|\mathbf{w}|_{k+1}|||\mathbf{v}|||.$$

We have proved the lemma. □

Theorem 5.1 *Let $(\boldsymbol{u},p)\in\boldsymbol{H}_0^1(\Omega)\cap\boldsymbol{H}^{k+1}(\Omega)\times(L_0^2(\Omega)\cap H^k(\Omega))$ with $k\ge 1$ and $(\boldsymbol{u}_h,p_h)\in V_h\times W_h$ be the solution of (1)-(3) and (11)-(12), respectively. Then, the following error estimates hold true*

$$|||\boldsymbol{u}-\boldsymbol{u}_h|||\le Ch^k|\boldsymbol{u}|_{k+1},\tag{40}$$

$$\|Q_hp-p_h\|\le Ch^k|\boldsymbol{u}|_{k+1},\tag{41}$$

$$\|p-p_h\|\le Ch^k(|\boldsymbol{u}|_{k+1}+|p|_k).\tag{42}$$

Proof By letting $\mathbf{v}=\mathbf{e}_h$ in (23) and $q=\varepsilon_h$ in (24) and adding the two resulting equations, we have

$$|||\mathbf{e}_h|||^2=|\ell_1(\mathbf{u},\mathbf{v})-\ell_2(\mathbf{u},\mathbf{v})|.\tag{43}$$

It then follows from (37) and (38) that

$$|||\mathbf{e}_h|||^2\le Ch^k|\mathbf{u}|_{k+1}|||\mathbf{e}_h|||.\tag{44}$$

By the triangle inequality and (44), (40) holds. To estimate $\|\varepsilon_h\|$, we have from (23) that

$$(\varepsilon_h,\nabla\cdot\mathbf{v})=(\nabla_w\mathbf{e}_h,\nabla_w\mathbf{v})-\ell_1(\mathbf{u},\mathbf{v})+\ell_2(\mathbf{u},\mathbf{v}).$$

Using the equation above (44) and (37), we arrive at

$$|(\varepsilon_h,\nabla\cdot\mathbf{v})|\le Ch^k|\mathbf{u}|_{k+1}|||\mathbf{v}|||.$$

Combining the above estimate with the *inf-sup* condition (20) gives

$$\|\varepsilon_h\|\le Ch^k|\mathbf{u}|_{k+1},$$

which yields the desired estimate (41). (42) follows by the triangle inequality. □

6 Error estimates in L^2 norm

In this section, we shall derive an L^2-error estimate for the velocity approximation through a duality argument. Recall that $\mathbf{e}_h=\Pi_h\mathbf{u}-\mathbf{u}_h$ and $\boldsymbol{\epsilon}_h=\mathbf{u}-\mathbf{u}_h$. To this end, consider the problem of seeking $(\boldsymbol{\psi}, \xi)$ such that

$$-\Delta\boldsymbol{\psi} + \nabla\xi = \boldsymbol{\epsilon}_h \quad \text{in } \Omega, \tag{45}$$

$$\nabla\cdot\boldsymbol{\psi} = 0 \quad \text{in } \Omega, \tag{46}$$

$$\boldsymbol{\psi} = 0 \quad \text{on } \partial\Omega. \tag{47}$$

Assume that the dual problem has the $\boldsymbol{H}^2(\Omega)\times H^1(\Omega)$-regularity property in the sense that the solution $(\boldsymbol{\psi}, \xi) \in \boldsymbol{H}^2(\Omega)\times H^1(\Omega)$ and the following a priori estimate holds true:

$$\|\boldsymbol{\psi}\|_2 + \|\xi\|_1 \le C\|\boldsymbol{\epsilon}_h\|. \tag{48}$$

Theorem 6.1 *Let $(\boldsymbol{u}_h, p_h) \in V_h \times W_h$ be the solution of (11)–(12). Assume that (48) holds true. Then, we have*

$$\|\boldsymbol{u} - \boldsymbol{u}_h\| \le Ch^{k+1}|\boldsymbol{u}|_{k+1}. \tag{49}$$

Proof Testing (45) by $\boldsymbol{\epsilon}_h$ gives

$$(\boldsymbol{\epsilon}_h, \boldsymbol{\epsilon}_h) = -(\Delta\boldsymbol{\psi},\ \boldsymbol{\epsilon}_h) + (\nabla\xi,\ \boldsymbol{\epsilon}_h). \tag{50}$$

Using integration by parts and the fact $\langle\nabla\boldsymbol{\psi}\cdot\mathbf{n}, \{\boldsymbol{\epsilon}_h\}\rangle_{\partial\mathcal{T}_h} = 0$, then

$$\begin{aligned}
-(\Delta\boldsymbol{\psi}, \boldsymbol{\epsilon}_h) &= (\nabla\boldsymbol{\psi},\ \nabla\boldsymbol{\epsilon}_h)_{\mathcal{T}_h} - \langle\nabla\boldsymbol{\psi}\cdot\mathbf{n},\ \boldsymbol{\epsilon}_h - \{\boldsymbol{\epsilon}_h\}\rangle_{\partial\mathcal{T}_h}\\
&= (\mathbb{Q}_h\nabla\boldsymbol{\psi},\ \nabla\boldsymbol{\epsilon}_h)_{\mathcal{T}_h} + (\nabla\boldsymbol{\psi} - \mathbb{Q}_h\nabla\boldsymbol{\psi},\ \nabla\boldsymbol{\epsilon}_h)_{\mathcal{T}_h} - \langle\nabla\boldsymbol{\psi}\cdot\mathbf{n},\ \boldsymbol{\epsilon}_h - \{\boldsymbol{\epsilon}_h\}\rangle_{\partial\mathcal{T}_h}\\
&= -(\nabla\cdot\mathbb{Q}_h\nabla\boldsymbol{\psi},\ \boldsymbol{\epsilon}_h)_{\mathcal{T}_h} + \langle\mathbb{Q}_h\nabla\boldsymbol{\psi}\cdot\mathbf{n},\ \boldsymbol{\epsilon}_h\rangle_{\partial\mathcal{T}_h}\\
&+ (\nabla\boldsymbol{\psi} - \mathbb{Q}_h\nabla\boldsymbol{\psi},\ \nabla\boldsymbol{\epsilon}_h)_{\mathcal{T}_h} - \langle\nabla\boldsymbol{\psi}\cdot\mathbf{n},\ \boldsymbol{\epsilon}_h - \{\boldsymbol{\epsilon}_h\}\rangle_{\partial\mathcal{T}_h}\\
&= (\mathbb{Q}_h\nabla\boldsymbol{\psi},\ \nabla_w\boldsymbol{\epsilon}_h)_{\mathcal{T}_h} + \langle\mathbb{Q}_h\nabla\boldsymbol{\psi}\cdot\mathbf{n},\ \boldsymbol{\epsilon}_h - \{\boldsymbol{\epsilon}_h\}\rangle_{\partial\mathcal{T}_h}\\
&+ (\nabla\boldsymbol{\psi} - \mathbb{Q}_h\nabla\boldsymbol{\psi},\ \nabla\boldsymbol{\epsilon}_h)_{\mathcal{T}_h} - \langle\nabla\boldsymbol{\psi}\cdot\mathbf{n},\ \boldsymbol{\epsilon}_h - \{\boldsymbol{\epsilon}_h\}\rangle_{\partial\mathcal{T}_h}\\
&= (\mathbb{Q}_h\nabla\boldsymbol{\psi},\ \nabla_w\boldsymbol{\epsilon}_h)_{\mathcal{T}_h} + (\nabla\boldsymbol{\psi} - \mathbb{Q}_h\nabla\boldsymbol{\psi},\ \nabla\boldsymbol{\epsilon}_h)_{\mathcal{T}_h} - \ell_1(\boldsymbol{\psi}, \boldsymbol{\epsilon}_h).
\end{aligned}$$

It follows from (13) that

$$\begin{aligned}
(\mathbb{Q}_h\nabla\boldsymbol{\psi},\ \nabla_w\boldsymbol{\epsilon}_h)_{\mathcal{T}_h} &= (\nabla_w\boldsymbol{\psi},\ \nabla_w\boldsymbol{\epsilon}_h)_{\mathcal{T}_h}\\
&= (\nabla_w\Pi_h\boldsymbol{\psi},\ \nabla_w\boldsymbol{\epsilon}_h)_{\mathcal{T}_h} + (\nabla_w(\boldsymbol{\psi} - \Pi_h\boldsymbol{\psi}),\ \nabla_w\boldsymbol{\epsilon}_h)_{\mathcal{T}_h}.
\end{aligned}$$

The two equations above imply that

$$\begin{aligned}
-(\Delta\boldsymbol{\psi}, \boldsymbol{\epsilon}_h) &= (\nabla_w\Pi_h\boldsymbol{\psi},\ \nabla_w\boldsymbol{\epsilon}_h)_{\mathcal{T}_h} + (\nabla_w(\boldsymbol{\psi} - \Pi_h\boldsymbol{\psi}),\ \nabla_w\boldsymbol{\epsilon}_h)_{\mathcal{T}_h}\\
&+ (\nabla\boldsymbol{\psi} - \mathbb{Q}_h\nabla\boldsymbol{\psi},\ \nabla\boldsymbol{\epsilon}_h)_{\mathcal{T}_h} - \ell_1(\boldsymbol{\psi}, \boldsymbol{\epsilon}_h).
\end{aligned} \tag{51}$$

It follows from integration by parts and (2) and (12)

$$(\nabla\xi,\ \boldsymbol{\epsilon}_h) = 0. \tag{52}$$

Equation (33) and the fact $(\epsilon_h, \nabla\cdot\Pi_h\boldsymbol{\psi})_{\mathcal{T}_h} = 0$ give

$$(\nabla_w\Pi_h\boldsymbol{\psi},\ \nabla_w\boldsymbol{\epsilon}_h)_{\mathcal{T}_h} = \ell_1(\mathbf{u}, \Pi\boldsymbol{\psi}_h). \tag{53}$$

Combining (50)–(53), we have

$$\begin{aligned}
\|\boldsymbol{\epsilon}_h\|^2 &= \ell_1(\mathbf{u}, \Pi_h\boldsymbol{\psi}) + (\nabla_w(\boldsymbol{\psi} - \Pi_h\boldsymbol{\psi}),\ \nabla_w\boldsymbol{\epsilon}_h)_{\mathcal{T}_h}\\
&+ (\nabla\boldsymbol{\psi} - \mathbb{Q}_h\nabla\boldsymbol{\psi},\ \nabla\boldsymbol{\epsilon}_h)_{\mathcal{T}_h} - \ell_1(\boldsymbol{\psi}, \boldsymbol{\epsilon}_h).
\end{aligned} \tag{54}$$

Next, we will estimate all the terms on the right hand side of (54). Using the Cauchy-Schwarz inequality, the trace inequality (14) and the definitions of Π_h and $\mathbb{Q}_h$ we obtain

$$\begin{aligned}
|\ell_1(\mathbf{u}, \Pi_h\boldsymbol{\psi})| &\le \left|\langle(\nabla\mathbf{u} - \mathbb{Q}_h\nabla\mathbf{u})\cdot\mathbf{n},\ \Pi_h\boldsymbol{\psi} - \{\Pi_h\boldsymbol{\psi}\}\rangle_{\partial T_h}\right| \\
&\le \left(\sum_{T\in\mathcal{T}_h}\|\nabla\mathbf{u} - \mathbb{Q}_h\nabla\mathbf{u}\|_{\partial T}^2\right)^{1/2}\left(\sum_{T\in\mathcal{T}_h}\|\Pi_h\boldsymbol{\psi} - \{\Pi_h\boldsymbol{\psi}\}\|_{\partial T}^2\right)^{1/2} \\
&\le C\left(\sum_{T\in\mathcal{T}_h}h\|\nabla\mathbf{u} - \mathbb{Q}_h\nabla\mathbf{u}\|_{\partial T}^2\right)^{1/2}\left(\sum_{T\in\mathcal{T}_h}h^{-1}\|[\Pi_h\boldsymbol{\psi} - \boldsymbol{\psi}]\|_{\partial T}^2\right)^{1/2} \\
&\le Ch^{k+1}|\mathbf{u}|_{k+1}|\boldsymbol{\psi}|_2.
\end{aligned}$$

It follows from (39) and (40) that

$$\begin{aligned}
|(\nabla_w(\boldsymbol{\psi} - \Pi_h\boldsymbol{\psi}),\ \nabla_w\boldsymbol{\epsilon}_h)_{\mathcal{T}_h}| &\le C|||\boldsymbol{\epsilon}_h|||\,|||\boldsymbol{\psi} - \Pi_h\boldsymbol{\psi}||| \\
&\le Ch^{k+1}|\mathbf{u}|_{k+1}|\boldsymbol{\psi}|_2.
\end{aligned}$$

The norm equivalence (17) and (40) imply

$$\begin{aligned}
|(\nabla\boldsymbol{\psi} - \mathbb{Q}_h\nabla\boldsymbol{\psi},\ \nabla\boldsymbol{\epsilon}_h)_{\mathcal{T}_h}| &\le C\left(\sum_{T\in\mathcal{T}_h}\|\nabla\boldsymbol{\epsilon}_h\|_T^2\right)^{1/2}\left(\sum_{T\in\mathcal{T}_h}\|\nabla\boldsymbol{\psi} - \mathbb{Q}_h\nabla\boldsymbol{\psi}\|_T^2\right)^{1/2} \\
&\le C\left(\sum_{T\in\mathcal{T}_h}(\|\nabla(\mathbf{u} - \Pi_h\mathbf{u})\|_T^2 + \|\nabla(\Pi_h\mathbf{u} - \mathbf{u}_h)\|_T^2)\right)^{1/2} \\
&\quad\times\left(\sum_{T\in\mathcal{T}_h}\|\nabla\boldsymbol{\psi} - \mathbb{Q}_h\nabla\boldsymbol{\psi}\|_T^2\right)^{1/2} \\
&\le Ch|\boldsymbol{\psi}|_2(h^k|\mathbf{u}|_{k+1} + |||\Pi_h\mathbf{u} - \mathbf{u}_h|||) \\
&\le Ch^{k+1}|\mathbf{u}|_{k+1}|\boldsymbol{\psi}|_2.
\end{aligned}$$

Using (17) and (40), we obtain

$$\begin{aligned}
|\ell_1(\boldsymbol{\psi}, \boldsymbol{\epsilon}_h)| &= \left|\langle(\nabla\boldsymbol{\psi} - \mathbb{Q}_h\nabla\boldsymbol{\psi})\cdot\mathbf{n},\ \boldsymbol{\epsilon}_h - \{\boldsymbol{\epsilon}_h\}\rangle_{\partial\mathcal{T}_h}\right| \\
&\le \sum_{T\in\mathcal{T}_h}h_T^{1/2}\|\nabla\boldsymbol{\psi} - \mathbb{Q}_h\nabla\boldsymbol{\psi}\|_{\partial T}h_T^{-1/2}\|[\boldsymbol{\epsilon}_h]\|_{\partial T} \\
&\le Ch\|\boldsymbol{\psi}\|_2\left(\sum_{T\in\mathcal{T}_h}h_T^{-1}(\|[\mathbf{e}_h]\|_{\partial T}^2 + \|[\mathbf{u} - \Pi_h\mathbf{u}]\|_{\partial T}^2\right)^{1/2} \\
&\le Ch\|\boldsymbol{\psi}\|_2(|||\mathbf{e}_h||| + \left(\sum_{T\in\mathcal{T}_h}h_T^{-1}\|[\mathbf{u} - \Pi_h\mathbf{u}]\|_{\partial T}^2\right)^{1/2} \\
&\le Ch^{k+1}|\mathbf{u}|_{k+1}\|\boldsymbol{\psi}\|_2.
\end{aligned}$$

Combining all the estimates above with (54) yields

$$\|\boldsymbol{\epsilon}_h\|^2 \leq Ch^{k+1}|\mathbf{u}|_{k+1}\|\boldsymbol{\psi}\|_2.$$

The estimate (49) follows from the above inequality and the regularity assumption (48). We have completed the proof. □

7 Numerical experiments

7.1 Example

Consider problem (1)– (3) with $\Omega = (0,1)^2$. The source term and the boundary value $\mathbf{g}$ are chosen so that the exact solution is

$$\mathbf{u}(x,y) = \begin{pmatrix} -(2-4y)(y-y^2)(x-x^2)^2 \\ (2-4x)(x-x^2)(y-y^2)^2 \end{pmatrix},$$
$$p = (2-4x)(x-x^2)(2-4y)(y-y^2).$$

In this example, we use uniform triangular grids as shown in Fig. 1. In Table 1, we list the errors and the orders of convergence. We can see that the optimal order of convergence is achieved in all finite elements.

7.2 Example

This example is from Example 1.1 in [10], for testing the pressure robustness of the method. We solve the following Stokes equations with a different Reynolds number $\mu^{-1} > 0$,

$$\begin{aligned} -\mu\Delta\mathbf{u} + \nabla p &= \begin{pmatrix} 3(x-x^2) - \frac{1}{2} \\ 0 \end{pmatrix} && \text{in } \Omega, \\ \nabla\cdot\mathbf{u} &= 0 && \text{in } \Omega, \\ \mathbf{u} &= \mathbf{0} && \text{on } \partial\Omega, \end{aligned}$$

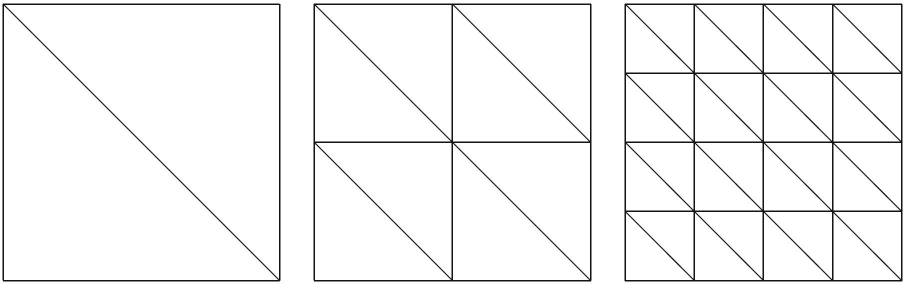

Fig. 1 The first three levels of triangular grids for Examples 7.1 and 7.2

Table 1 Example 7.1: Error profiles and convergence rates on grids as shown in Fig. 1

Level	$\|\mathbf{u}-\mathbf{u}_h\|_0$	Rate	$\|\!\|\mathbf{u}-\mathbf{u}_h\|\!\|$	Rate	$\|p-p_h\|_0$	Rate
	by the P_1^2-P_0 $H(\text{div})$ element (6)–(7)					
5	0.6699E−01	1.82	0.3105E+01	1.05	0.1087E+01	1.12
6	0.1754E−01	1.93	0.1516E+01	1.03	0.5164E+00	1.07
7	0.4468E−02	1.97	0.7479E+00	1.02	0.2528E+00	1.03
	by the P_2^2-P_1 $H(\text{div})$ element (6)–(7)					
5	0.7769E−03	3.10	0.1607E+00	1.95	0.3320E+00	1.68
6	0.9439E−04	3.04	0.4059E−01	1.98	0.9258E−01	1.84
7	0.1170E−04	3.01	0.1018E−01	2.00	0.2443E−01	1.92
	by the P_3^2-P_2 $H(\text{div})$ element (6)–(7)					
4	0.3821E−03	3.90	0.4483E−01	2.80	0.1374E+00	2.71
5	0.2444E−04	3.97	0.5895E−02	2.93	0.1884E−01	2.87
6	0.1550E−05	3.98	0.7560E−03	2.96	0.2461E−02	2.94
	by the P_4^2-P_3 $H(\text{div})$ element (6)–(7)					
4	0.2350E−04	4.85	0.3140E−02	3.81	0.5804E−02	3.85
5	0.7645E−06	4.94	0.2082E−03	3.91	0.3818E−03	3.93
6	0.2433E−07	4.97	0.1341E−04	3.96	0.2447E−04	3.96

Table 2 Example 7.2: Error profiles and convergence rates (P_2) on grids as shown in Fig. 1

Level	$\|\mathbf{I}_h\mathbf{u}-\mathbf{u}_h\|_0$	Rate	$\|\mathbf{I}_h\mathbf{u}-\mathbf{u}_h\|_{1,h}$	Rate	$\|I_h p-p_h\|_0$	Rate
	by the P_2^2-P_1 Taylor-Hood element, $\mu=1$					
5	0.2292E−06	3.99	0.2733E−04	2.93	0.9301E−03	1.89
6	0.1438E−07	3.99	0.3491E−05	2.97	0.2413E−03	1.95
7	0.9002E−09	4.00	0.4410E−06	2.98	0.6148E−04	1.97
	by the P_2^2-P_1 Taylor-Hood element, $\mu=10^{-6}$					
5	0.2292E+00	3.99	0.2733E+02	2.93	0.9301E−03	1.89
6	0.1438E−01	3.99	0.3491E+01	2.97	0.2413E−03	1.95
7	0.9002E−03	4.00	0.4410E+00	2.98	0.6148E−04	1.97
	by the P_2^2-P_1 $H(\text{div})$ element (6)–(7), $\mu=1$					
5	0.1224E−18	−−	0.1674E−17	−−	0.5615E−03	1.94
6	0.1032E−18	−−	0.1813E−17	−−	0.1434E−03	1.97
7	0.1002E−18	−−	0.1830E−17	−−	0.3624E−04	1.98
	by the P_2^2-P_1 $H(\text{div})$ element (6)–(7), $\mu=10^{-6}$					
5	0.1032E−12	−−	0.1554E-11	−−	0.5615E−03	1.94
6	0.6375E−13	−−	0.1627E-11	−−	0.1434E−03	1.97
7	0.9934E−13	−−	0.1760E-11	−−	0.3624E−04	1.98

Accepted Manuscript
Version of record at: https://doi.org/10.1007/s10444-021-09856-9

Table 3 Example 7.2: Error profiles and convergence rates (P_3) on grids as shown in Fig. 1

Level	$\|\mathbf{I}_h\mathbf{u}-\mathbf{u}_h\|_0$	Rate	$\|\mathbf{I}_h\mathbf{u}-\mathbf{u}_h\|_{1,h}$	Rate	$\|I_hp-p_h\|_0$	Rate
	by the P_3^2-P_2 Taylor-Hood element, $\mu=1$					
4	0.7690E−06	3.64	0.4897E−04	2.74	0.5746E−04	3.09
5	0.5345E−07	3.85	0.6637E−05	2.88	0.6828E−05	3.07
6	0.3509E−08	3.93	0.8620E−06	2.94	0.8275E−06	3.04
	by the P_3^2-P_2 Taylor-Hood element, $\mu=10^{-6}$					
4	0.7690E+00	3.64	0.4897E+02	2.74	0.5746E−04	3.09
5	0.5345E−01	3.85	0.6637E+01	2.88	0.6828E−05	3.07
6	0.3509E−02	3.93	0.8620E+00	2.94	0.8275E−06	3.04
	by the P_3^2-P_2 $H(\text{div})$ element (6)–(7), $\mu=1$					
4	0.1699E−17	−−	0.1801E−16	−−	0.5580E−04	3.00
5	0.1403E−17	−−	0.1486E−16	−−	0.6975E−05	3.00
6	0.3710E−18	−−	0.7074E−17	−−	0.8719E-06	3.00
	by the P_3^2-P_2 $H(\text{div})$ element (6)–(7), $\mu=10^{-6}$					
4	0.1655E−11	−−	0.1789E−10	−−	0.5580E−04	3.00
5	0.1318E−11	−−	0.1449E−10	−−	0.6975E−05	3.00
6	0.3331E−12	−−	0.6899E−11	−−	0.8719E−06	3.00

where $\Omega=(0,1)^2$. The exact solution is, independent of μ,

$$\mathbf{u}=\begin{pmatrix}0\\0\end{pmatrix},\qquad p=(x-x^2)(x-\tfrac{1}{2}). \tag{55}$$

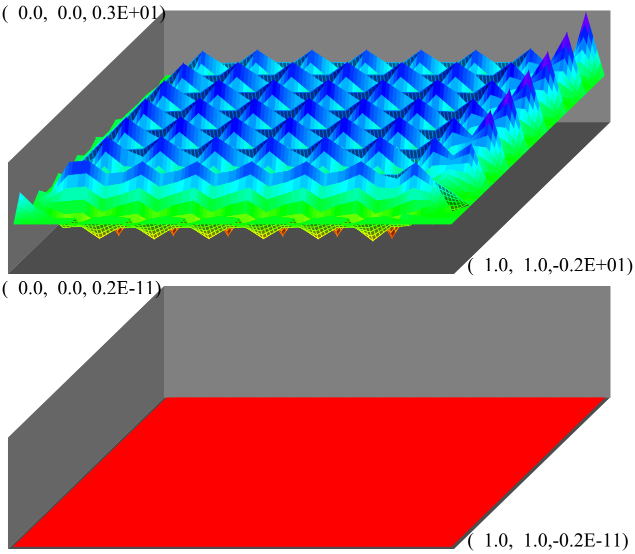

Fig. 2 The solution $(\mathbf{u}_h)_1$ of the P_3 Taylor-Hood element (top) and the P_3 $H(\text{div})$ element (bottom), on the 4th level grid, for $\mu=10^{-6}$

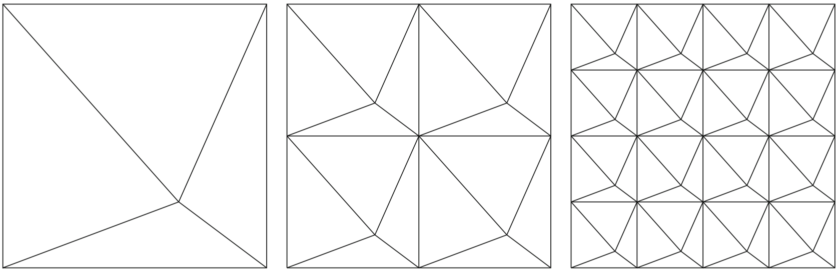

Fig. 3 The first three grids for the computation of Example 7.3

For this problem, a non-pressure-robust method, such as the Taylor-Hood method, would produce a μ-dependent velocity solution, cf. the numerical results in [10] and the data in Tables 2 and 3 below.

In this example, we use uniform grids as shown in Fig. 1. In Tables 2 and 3, we list the errors and the orders of convergence for both the $H(\mathrm{div})$ finite element and the Taylor-Hood element. We can see that the discrete velocity solution u_h is identically zero for our method (only computer round-off error), i.e., of optimal order convergence independently of μ. But its error is $\mu^{-1}O(h^k)$ for the Taylor-Hood element. For P_2 Taylor-Hood element, there is one order superconvergence in both L^2-norm and H^1-semi-norm, noting $\mathbf{u} = \mathbf{0}$ here. But there is no such superconvergence for P_k $H(\mathrm{div})$ elements, neither for P_3 Taylor-Hood element. To show the pollution effect of the Taylor-Hood element, we plot two solutions in Fig. 2.

Table 4 Example 7.3: Error profiles and convergence rates (P_2) on grids as shown in Fig. 3

Level	$\|\mathbf{I}_h\mathbf{u} - \mathbf{u}_h\|_0$	Rate	$\|\mathbf{I}_h\mathbf{u} - \mathbf{u}_h\|_{1,h}$	Rate	$\|I_h p - p_h\|_0$	Rate
	by the P_2^2-P_1 Taylor-Hood element, $\mu = 1$					
4	0.8795E−05	3.09	0.5572E−03	2.01	0.1943E−02	1.85
5	0.1080E−05	3.03	0.1393E−03	2.00	0.5115E−03	1.93
6	0.1348E−06	3.00	0.3493E−04	2.00	0.1312E−03	1.96
	by the P_2^2-P_1 Taylor-Hood element, $\mu = 10^{-6}$					
4	0.8795E+01	3.09	0.5572E+03	2.01	0.1943E−02	1.85
5	0.1080E+01	3.03	0.1393E+03	2.00	0.5115E−03	1.93
6	0.1348E+00	3.00	0.3493E+02	2.00	0.1312E−03	1.96
	by the P_2^2-P_1 $H(\mathrm{div})$ element (6)–(7), $\mu = 1$					
4	0.2442E−16	– –	0.2637E−15	– –	0.4478E−02	1.84
5	0.8580E−17	– –	0.2774E−15	– –	0.1178E−02	1.93
6	0.2622E−16	– –	0.2874E−15	– –	0.3019E−03	1.96
	by the P_2^2-P_1 $H(\mathrm{div})$ element (6)–(7), $\mu = 10^{-6}$					
4	0.2540E−10	– –	0.2697E−12	– –	0.4478E−02	1.84
5	0.8075E−11	– –	0.2760E−12	– –	0.1178E−02	1.93
6	0.2625E−10	– –	0.2876E−12	– –	0.3019E−03	1.96

Table 5 Example 7.3: Error profiles and convergence rates (P_3) on grids as shown in Fig. 3

Level	$\|\mathbf{I}_h\mathbf{u}-\mathbf{u}_h\|_0$	Rate	$\|\mathbf{I}_h\mathbf{u}-\mathbf{u}_h\|_{1,h}$	Rate	$\|I_h p - p_h\|_0$	Rate
	by the P_3^2-P_2 Taylor-Hood element, $\mu = 1$					
4	0.2272E−06	3.79	0.1912E−04	2.84	0.1463E−03	3.00
5	0.1516E−07	3.91	0.2515E−05	2.93	0.1826E−04	3.00
6	0.9770E−09	3.96	0.3221E−06	2.96	0.2281E−05	3.00
	by the P_3^2-P_2 Taylor-Hood element, $\mu = 10^{-6}$					
4	0.2272E+00	3.79	0.1912E+02	2.84	0.1463E−03	3.00
5	0.1516E−01	3.91	0.2515E+01	2.93	0.1826E−04	3.00
6	0.9770E−03	3.96	0.3221E+00	2.96	0.2281E−05	3.00
	by the P_3^2-P_2 $H(\text{div})$ element (6)–(7), $\mu = 1$					
4	0.1356E−12	−−	0.5899E−11	−−	0.1343E−03	3.00
5	0.1375E−12	−−	0.3215E−11	−−	0.1679E−04	3.00
6	0.1401E−12	−−	0.2179E−11	−−	0.2099E−05	3.00
	by the P_3^2-P_2 $H(\text{div})$ element (6)–(7), $\mu = 10^{-6}$					
4	0.1360E−06	−−	0.5903E−08	−−	0.1343E−03	3.00
5	0.1377E−06	−−	0.3217E−08	−−	0.1679E−04	3.00
6	0.1395E−06	−−	0.2053E−08	−−	0.2099E−05	3.00

7.3 Example

In this example, we compute the problem in Example 7.2 again, i.e., we compute the numerical solution for (55) on irregular grids as shown in Fig. 3.

In Tables 4 and 5, we list the errors and the orders of convergence for both the Taylor-Hood element and the $H(\text{div})$ finite element. We can see that the discrete velocity solution u_h is still zero up to computer accuracy, on irregular grids. But as expected, the error for approximating the velocity is $\mu^{-1}O(h^k)$ for the Taylor-Hood element. Unlike Example 7.2, the P_2 Taylor-Hood element does not have any superconvergence on irregular grids.

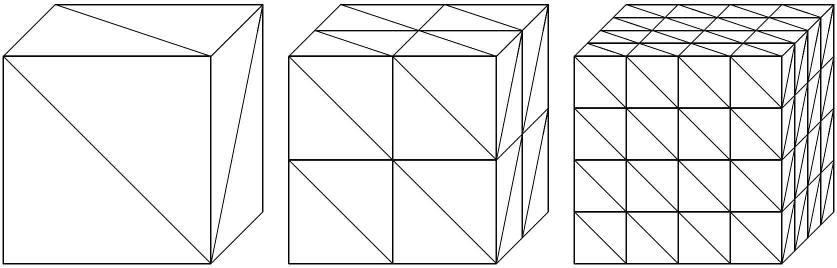

Fig. 4 The first three levels of grids used in Example 7.4

Table 6 Example 7.4: Error profiles and convergence rates on 3D grids as shown in Fig. 4

Grid	$\|\|\|\mathbf{u}-\mathbf{u}_h\|\|\|$	Rate	$\|\mathbf{u}-\mathbf{u}_h\|_0$	Rate	$\|p-p_h\|_0$	Rate
1	0.2599E+00	0.00	0.1654E−01	0.00	0.6503E+00	0.00
2	0.2155E+00	0.27	0.1091E−01	0.60	0.3843E+00	0.76
3	0.1212E+00	0.83	0.3520E−02	1.63	0.1232E+00	1.64
4	0.6209E−01	0.97	0.1006E−02	1.81	0.3879E−01	1.67

7.4 Example

Consider problem (1) with $\Omega = (0, 1)^3$. The source term f and the boundary value g are chosen so that the exact solution is

$$\mathbf{u}(x, y, z) = \begin{pmatrix} y^2 \\ z^2 \\ x^2 \end{pmatrix}, \quad p(x, y, z) = yz - \frac{1}{4}.$$

We use uniform tetrahedral meshes as shown in Fig. 4. The results of the method of the P_2^2-P_1 $H(\mathrm{div})$ element (6)– (7) are listed in Table 6. The method converges at the optimal order in the usual norms.

Funding Xiu Ye was supported in part by the National Science Foundation Grant DMS-1620016.

References

1. Al-Taweel, A., Wang, X.: A note on the optimal degree of the weak gradient of the stabilizer free weak Galerkin finite element method. Appl. Numer. Math. **150**, 444–451 (2020)
2. Brenner, S., Scott, L. The mathematical theory of finite element methods, 3rd edn. Springer, Berlin (2008)
3. Brezzi, F., Fortin, M.: Mixed and hybrid finite elements. Springer-Verlag, New York (1991)
4. Chen, W., Wang, F., Wang, Y.: Weak Galerkin method for the coupled Darcy–Stokes flow. IMA . Numer. Anal **36**, 897–921 (2016)
5. Chen, G., Feng, M., Xie, X.: Robust globally divergence-free weak Galerkin methods for Stokes equations. J. Comput. Math. **34**, 549–572 (2016)
6. Cockburn, B., Kanschat, G., Schotzau, D.: A note on discontinuous galerkin divergence-free solutions of the navier-stokes equations. J. Sci. Comp. **31**, 61–73 (2007)
7. Crouzeix, M., Raviart, P.: Conforming and nonconforming finite element methods for solving the stationary Stokes equations. RAIRO Anal. Numer. **7**, 33–76 (1973)
8. Falk, R., Neilan, M.: Stokes complexes and the construction of stable finite element methods with pointwise mass conservation. SIAM J. Numer. Anal. **51**, 1308–1326 (2013)
9. Girault, V., Raviart, P.: Finite element methods for the navier-stokes equations: theory and algorithms. Springer-Verlag, Berlin (1986)
10. John, V., Linke, A., Merdon, C., Neilan, M., Rebholz, L.: On the divergence constraint in mixed finite element methods for incompressible flows. SIAM Rev.w **59**, 492–544 (2017)
11. Lehrenfeld, C., Schoberl, J.: High order exactly divergence-free hybrid discontinuous Galerkin methods for unsteady incompressible flows. Comput. Method. Appl. Mech. Eng. **307**, 339–361 (2016)
12. Li, R., Li, J., Liu, X., Chen, Z.: A weak Galerkin finite element method for a coupled Stokes-Darcy problem. Numer. Meth. Part. Diff. Eq. **33**, 111-127 (2017)

Accepted Manuscript
Version of record at: https://doi.org/10.1007/s10444-021-09856-9

13. Linke, A., Merdon, C.: Pressure-robustness and discrete Helmholtz projectors in mixed finite element methods for the incompressible Navier–Stokes equations. Comput. Method. Appl. Mech. Eng **311**, 304–326 (2016)
14. Mu, L., Wang, X., Ye, X.: A modified weak Galerkin finite element method for the Stokes equations. J. Comput. Appl. Math. **275**, 79–90 (2015)
15. Schotzau, D., Schwab, C., Toselli, A.: Mixed hp-DGFEM for incompressible flows. SIAM J. Numer. Anal. **40**, 2171–2194 (2003)
16. Scott, L., Vogelius, M.: Norm estimates for a maximal right inverse of the divergence operator in spaces of piecewise polynomials. ESAIM: M2AN **19**, 111–143 (1985)
17. Tian, T., Zhai, Q., Zhang, R.: A new modified weak Galerkin finite element scheme for solving the stationary Stokes equations. J. Comput. Appl. Math. **329**, 268–279 (2018)
18. Wang, J., Wang, Y., Ye, X.: A robust numerical method for Stokes equations based on divergence-free H(div) finite element methods. SIAM J. Sci. Comput. **31**, 2784–2802 (2009)
19. Wang, J., Ye, X.: New finite element methods in computational fluid dynamics by H(div) elements. SIAM Numer. Anal. **45**, 1269–1286 (2007)
20. Wang, J., Ye, X.: A weak Galerkin finite element method for the Stokes equations. Adv. Comput. Math. **42**, 155–174 (2016)
21. Wang, J., Ye, X.: A weak Galerkin finite element method for second-order elliptic problems. J. Comput. Appl. Math. **241**, 103–115 (2013)
22. Wang, J., Ye, X.: A Weak Galerkin mixed finite element method for second-order elliptic problems. Math. Comp. **83**, 2101–2126 (2014)
23. Zhang, S.: Divergence-free finite elements on tetrahedral grids for $k \geq 6$. Math. Comput. **80**, 669–695 (2011)